An Implicit DGTD Method for Solving the Two-Dimensional Maxwell Equations on Unstructured Triangular Meshes

Adrien Catella, Victorita Dolean, Stephane Lanteri

INRIA

INSTITUT NATIONAL DE RECHERCHE EN INFORMATIQUE ET EN AUTOMATIQUE

An Implicit DGTD Method for Solving the Two-Dimensional Maxwell Equations on Unstructured Triangular Meshes

Adrien Catella — Victorita Dolean — Stéphane Lanteri

N° 6106

Janvier 2007

Thème NUM

ISSN 0249-6399 ISRN INRIA/RR--6106--FR+ENG

An Implicit DGTD Method for Solving the Two-Dimensional Maxwell Equations on Unstructured Triangular Meshes

Adrien Catella * , Victorita Dolean † , Stéphane Lanteri*

Thème NUM — Systèmes numériques
Projet Caiman

Rapport de recherche n° 6106 — Janvier 2007 — 29 pages

Abstract: Numerical methods for solving the time domain Maxwell equations often rely on cartesian meshes and are variants of the finite difference time domain method originating in the seminal work of Yee[23]. In the recent years, there has been an increasing interest in discontinuous Galerkin time domain methods dealing with unstructured meshes since the latter are particularly well suited for the discretization of geometrical details that characterize applications of practical relevance. Similarly to Yee's finite difference time domain method, discontinuous Galerkin time domain methods generally rely on explicit time integration schemes and are therefore constrained by a stability condition that can be very restrictive on highly refined or unstructured meshes and when the local approximation relies on high order polynomial interpolation. An implicit time integration scheme is a natural way to obtain a time domain method which is unconditionally stable. However, such a time scheme comes at the expense of the inversion of a global linear system at each time step, thus obliterating one of the attractive features of discontinuous Galerkin formulations. In this paper, we report on our recent efforts concerning the design of an implicit time integration scheme in conjunction with a discontinuous Galerkin approximation method for solving the time domain Maxwell equations on unstructured triangular meshes. Despite the memory and computational overheads induced by the inversion of a global linear system at each time step, we demonstrate that an implicit discontinuous Galerkin time domain method is a viable numerical strategy for solving electromagnetic wave propagation problems on locally refined unstructured meshes.

Key-words: computational electromagnetism, time domain Maxwell equations, discontinuous Galerkin methods, implicit time integration. unstructured meshes.

* INRIA Sophia Antipolis, project-team Caiman, 2004 Route des Lucioles, BP 93, F-06902 Sophia Antipolis Cedex, France

† University of Nice-Sophia Antipolis, J.A. Dieudonné Mathematics Laboratory, F-06108 Nice Cedex, France

Unité de recherche INRIA Sophia Antipolis
2004, route des Lucioles, BP 93, 06902 Sophia Antipolis Cedex (France)
Téléphone : +33 4 92 38 77 77 —Télécopie : +33 4 92 38 77 65

Une méthode de type Galerkin discontinu implicite pour la résolution numérique des équations de Maxwell 2D en domaine temporel sur des maillages triangulaires non-structurés

Résumé : La résolution numérique des équations de Maxwell en domaine temporel repose très souvent sur des méthodes en maillages cartésiens qui sont des variantes de la méthode différences finies initialement proposée par Yee[23]. Ces dernières années, un intérêt croissant a été porté aux méthodes de type Galerkin discontinu utilisant des maillages non-structurés ces derniers étant particulièrement bien adaptés à la discrétisation des détails géométriques qui caractérisent les applications réalistes. Comme dans la méthode différences finies de Yee, les méthodes de type Galerkin discontinu en domaine temporel font le plus souvent appel à des schémas d'intégration en temps explicites et sont soumises à des limites de stabilité qui s'avèrent contraignantes en maillages localement raffinés ou lorsque l'ordre d'interpolation local est élevé. Un schéma d'intégration implicite est une voie naturelle pour aboutir à une méthode numérique inconditionnellement stable. Cependant, un tel schéma conduit à la résolution d'un système linéaire à chaque pas de temps effaçant du même coup un des principaux avantages des formulations de type Galerkin discontinu. Nous présentons ici les résultats d'une étude visant à la mise au point d'une méthode de type Galerkin discontinu implicite en maillages triangulaires non-structurés pour la résolution numérique des équations de Maxwell 2D. Nous démontrons notamment qu'en dépit des surcoûts mémoire et computationnel induits par l'inversion d'un système linéaire à chaque pas de temps, une telle méthode conduit à une stratégie performante pour la simulation de problèmes de propagation d'ondes électromagnétiques en maillages localement raffinés.

Mots-clés : électromagnétisme numérique, équations de Maxwell en domaine temporel, méthodes Galerkin discontinues, intégration en temps implicite.

Contents

1 Introduction

In the numerical treatment of the time domain Maxwell equations, finite difference time domain (FDTD) methods based on Yee's scheme[23] are still prominent because of their simplicity (a time explicit method defined on Cartesian meshes) and their non-dissipative nature (they hold an energy conservation property which is an important ingredient in the numerical simulation of unsteady wave propagation problems). Unfortunately, when dealing with complex geometries, the FDTD method is not always the best choice since local refinements of the grid, albeit possible in the form of subgridding techniques [6], has an adverse effect on accuracy and efficiency. In particular, local refinement translates in a very restrictive time step in order to preserve the stability of the explicit leap-frog scheme used for time integration in the FDTD method. Finite element time domain (FETD) based on unstructured meshes can easily deal with complex geometries however they induce heavy computations or require accurate and efficient lumping of mass matrices [20]. Finite volume time domain (FVTD) methods on unstructured meshes also appeared as an alternative to FDTD methods, but they suffer from numerical diffusion resulting from the use of upwind schemes [8], and their extension to high-order accuracy is a tedious task.

A viable alternative to the aforementioned methods which has been knowing a remarkably vigorous development during the last decade is known as the discontinuous Galerkin method [1]-[2]-[3]. Originally devised for dealing with hyperbolic problems and largely adopted by the computational fluid dynamics community, this method is now applied to a variety of problems of practical interest and in particular, to the numerical resolution of the time domain Maxwell equations [15]-[9]-[7]- [13]-[17]-[21]. Discontinuous Galerkin time domain (DGTD) methods can be seen as high order generalizations of the FVTD methods, where the finite element approximation is piecewise constant inside elements. The different achievements of the FVTD methods are now being extended in the context of DGTD applications motivated by the ability of these methods to handle complicated geometries, media and meshes, to achieve a high order of accuracy by simply choosing suitable basis functions, to allow long-range time integrations and, last but not least, to remain highly parallelizable [5]. However, DGTD methods suffer from the same limitation concerning the allowable time step on locally refined unstructured meshes. Moreover, locally refined meshes induce numerical dispersion that may be corrected by local time-stepping strategies which is still an open problem in the framework of time domain numerical methods in general and the DGTD method in particular. Recently, promising solutions to local time-stepping strategies in combination with DGTD methods [22] have been proposed in the framework of symplectic time integration schemes.

An implicit time integration scheme is a natural route to a time domain method which is unconditionally stable. However, such a time scheme comes at the expense of the inversion of a global linear system at each time step, thus obliterating one of the attractive features of discontinuous Galerkin formulations. Nevertheless, an implicit time scheme can prove beneficial with regards to the stability restriction on the time step if used locally in regions where the underlying mesh is highly refined and if a stable explicit-implicit coupling can be

achieved. As a matter of fact, one of the methods proposed in [22] actually aims at combining explicit and implicit time integration schemes in a stable way (the resulting method can be seen as a locally implicit DGTD method). As a first step in this direction, we report here on our recent efforts concerning the design of a global implicit time integration scheme in conjunction with a discontinuous Galerkin approximation method for solving the time domain Maxwell equations on unstructured triangular meshes. Despite the memory and computational overheads induced by the inversion of a global linear system at each time step, we actually demonstrate that a globally implicit discontinuous Galerkin time domain method is a viable numerical strategy for solving electromagnetic wave propagation problems on locally refined unstructured triangular meshes. This is considered as a promising result in view of designing a globally or locally implicit DGTD method for solving the 3D Maxwell equations on tetrahedral meshes.

As mentioned previously, Yee's FDTD method has been the prevalent numerical strategy for solving the time domain Maxwell equations. A few implicit variants of this method have been developed among which, the alternating direction implicit finite difference time domain (ADI-FDTD) method [18] which is a non-dissipative implicit FDTD method. In [18], the authors demonstrate through numerical experiments that the ADI-FDTD method allows reductions in CPU times by a factor roughly equal to 4 as compared to the original FDTD method, for compatible levels of accuracy of the solutions of problems related to antenna design. Introduced more than fifty years ago for solving parabolic and elliptic partial differential equations [19], the ADI-FDTD method offers unconditional stability with modest computational overhead despite its implicit formulation. The ADI scheme is based on a factorization of the implicit matrix operator as $A = L_x L_y L_z$ where $L_{x,y,z}$ are tri-diagonal matrices that essentially correspond to the discretization of 1D problems in the x, y and z directions. A comprehensive analysis of the numerical dispersion of the ADI-FDTD method in the three-dimensional case is presented in [24] where it is shown that, on a non-uniform Cartesian mesh, the time step can be taken uniformly the same as that defined by the coarsest cell without altering the accuracy in the finer mesh regions. However, in [14], Garcia *at al.* exhibit accuracy limitations of the ADI-FDTD method that have not been revealed by studies on numerical dispersion, by investigating the truncation error on the time step due to the factorization. More precisely, the ADI-FDTD method is expressed as a $O(\Delta t^2)$ perturbation of an implicit Crank-Nicolson FDTD formulation and it is shown that some terms of the truncation error grow with the square of the time increment multiplied by the spatial derivatives of the fields, thus giving rise to potentially large numerical errors as the time step is increased.

Implicit time domain methods on general unstructured meshes have not been studied extensively so far. The main argument for not considering implicit time integration schemes in this context is that for each time iteration, a linear system must be solved which involves an irregularly structured sparse matrix, thus requiring a direct (LU-like) or preconditioned iterative procedure. Clearly, for three-dimensional problems, this can preclude the use of a time integration scheme. In this paper, we report on the results of a first step in this direction. We study and evaluate an implicit time integration scheme in conjunction with a

discontinuous Galerkin approximation method for solving the time domain Maxwell equations on unstructured triangular meshes. Despite the memory and computational overheads induced by the use of an implicit time integration scheme, we demonstrate the benefits of using such a scheme for time domain electromagnetic wave propagation problems on locally refined unstructured meshes. The proposed method is formulated in section 2 which also includes theoretical results concerning energy conservation and well-posedness of the discrete problem. The resulting implicit DGTD method is evaluated numerically in section 3 both in terms of accuracy and overall performance. Finally, section 4 concludes this study and states future research directions.

2 Implicit DGTD-$\mathbb{P}_p$ method

The starting point of this study is given by the explicit DGTD-$\mathbb{P}_p$ method presented in [13] for solving the three-dimensional time domain Maxwell equations on unstructured tetrahedral meshes. Beside a standard discontinuous Galerkin formulation, this method is based on two basic ingredients: a centered approximation for the computation of the numerical flux at inter-element boundaries, and an explicit leap-frog time integration scheme. The implicit DGTD-$\mathbb{P}_p$ method differs from its explicit counterpart in the time integration scheme which is now chosen to be a Crank-Nicolson scheme. The resulting implicit DGTD-$\mathbb{P}_p$ method is non-dissipative and unconditionally stable as will be shown in the sequel. Although the objective of this paper is to evaluate the proposed method in the context of the numerical resolution of the two-dimensional Maxwell equations, in this section we formulate and study the implicit DGTD-$\mathbb{P}_p$ method in the more general case of the three-dimensional case.

2.1 Formulation of the continuous problem

The system of time domain Maxwell equations in the absence of current sources is given by:

$$\begin{cases} \varepsilon \partial_t \mathbf{E} - \text{curl}(\mathbf{H}) = 0, \\ \mu \partial_t \mathbf{H} + \text{curl}(\mathbf{E}) = 0. \end{cases} \tag{1}$$

where $\mathbf{E}$ and $\mathbf{H}$ are the unknown electric and magnetic fields, ε and μ respectively denote the electric permittivity and the magnetic permeability (the propagation medium is assumed to be a linear and isotropic material). Our goal is to solve system (1) in a domain Ω of border $\partial\Omega = \Gamma_a \cup \Gamma_m$, where we impose the following boundary conditions:

$$\begin{cases} \mathbf{n} \times \mathbf{E} = 0 \text{ on } \Gamma_m, \\ \mathbf{n} \times \mathbf{E} - \sqrt{\dfrac{\mu}{\varepsilon}} \mathbf{n} \times (\mathbf{H} \times \mathbf{n}) = 0 \text{ on } \Gamma_a. \end{cases} \tag{2}$$

Here $\mathbf{n}$ denotes the unit outward normal to $\partial\Omega$. The first boundary condition is called *metallic* (referring to a perfectly conducting surface) while the second condition is called *absorbing*, takes the form of the Silver-Müler condition which is a first order approximation

of the exact absorbing boundary condition and is applied on Γ_a which represents the artificial limit of the computational domain.

Problem (1) can be rewritten under the following form:

$$\begin{cases} G_0\partial_t\mathbf{W} + G_x\partial_x\mathbf{W} + G_y\partial_y\mathbf{W} + G_z\partial_z\mathbf{W} = 0 \text{ in } \Omega, \\ (M_{\Gamma_m} - G_{\mathbf{n}})\mathbf{W} = 0 \text{ on } \Gamma_m, \\ (M_{\Gamma_a} - G_{\mathbf{n}})\mathbf{W} = 0 \text{ on } \Gamma_a. \end{cases} \tag{3}$$

where $\mathbf{W} = (\mathbf{E}, \mathbf{H})^t$ represents the electromagnetic field and matrix G_0 contains the properties of the media:

$$G_0 = \begin{pmatrix} \varepsilon\,\mathrm{Id}_3 & 0_{3\times3} \\ 0_{3\times3} & \mu\,\mathrm{Id}_3 \end{pmatrix},$$

where Id_k is the identity matrix of size k and $0_{l\times m}$ the $l \times m$ null matrix. Here G_l with $l \in \{x, y, z\}$ is such that $G_l\mathbf{W} = (\mathbf{H} \times \mathbf{e}_l, -\mathbf{E} \times \mathbf{e}_l)^t$, where $\mathbf{e}_l$ is an element of the canonical base of $\mathbb{R}^3$:

$$G_l = \begin{pmatrix} 0_{3\times3} & N_{\mathbf{e}_l} \\ N_{\mathbf{e}_l}^t & 0_{3\times3} \end{pmatrix},$$

while $G_{\mathbf{n}}$ is such that $G_{\mathbf{n}}\mathbf{W} = (\mathbf{H} \times \mathbf{n}, -\mathbf{E} \times \mathbf{n})^t$ and is given by:

$$G_{\mathbf{n}} = \begin{pmatrix} 0_{3\times3} & N_{\mathbf{n}} \\ N_{\mathbf{n}}^t & 0_{3\times3} \end{pmatrix} \text{ with } N_{\mathbf{n}} = \begin{pmatrix} 0 & \mathbf{n}_z & -\mathbf{n}_y \\ -\mathbf{n}_z & 0 & \mathbf{n}_x \\ \mathbf{n}_y & -\mathbf{n}_x & 0 \end{pmatrix}.$$

The matrices $G_{\mathbf{n}}^+$ and $G_{\mathbf{n}}^-$ are the negative and positive parts [1] of matrix $G_{\mathbf{n}}$. We define also $|G_{\mathbf{n}}| = G_{\mathbf{n}}^+ - G_{\mathbf{n}}^-$. Therefore $|G_{\mathbf{n}}|$ is given by:

$$|G_{\mathbf{n}}| = \begin{pmatrix} N_{\mathbf{n}}N_{\mathbf{n}}^t & 0_{3\times3} \\ 0_{3\times3} & N_{\mathbf{n}}^tN_{\mathbf{n}} \end{pmatrix}.$$

Finally, the matrices M_{Γ_m} and M_{Γ_a} are used for taking into account the metallic and absorbing boundary conditions:

$$M_{\Gamma_m} = \begin{pmatrix} 0_{3\times3} & N_{\mathbf{n}} \\ -N_{\mathbf{n}}^t & 0_{3\times3} \end{pmatrix} \text{ and } M_{\Gamma_a} = |G_{\mathbf{n}}|. \tag{4}$$

In particular, we note that $(M_{\Gamma_a} - G_{\mathbf{n}})\mathbf{W} = 0 \Leftrightarrow G_{\mathbf{n}}^-\mathbf{W} = 0$.

[1] If $G_{\mathbf{n}} = T\Lambda T^{-1}$ with Λ a diagonal matrix of eigenvalues of $G_{\mathbf{n}}$ then $G_{\mathbf{n}}^{\pm} = T\Lambda^{\pm}T^{-1}$ where Λ^+ (respectively Λ^-) contains the positive (respectively negative) eigenvalue of the matrix $G_{\mathbf{n}}$.

2.2 Semi-discretization in time

In this study, we discretize the system (3) with respect to the time variable using the Crank-Nicolson scheme:

$$G_0\left(\frac{\mathbf{W}^{n+1}-\mathbf{W}^n}{\Delta t}\right)+(G_x\partial_x+G_y\partial_y+G_z\partial_z)\left(\frac{\mathbf{W}^{n+1}+\mathbf{W}^n}{2}\right)=0 \tag{5}$$

where $\mathbf{W}^n$ is the approximation of $\mathbf{W}$ at time $t_n=n\Delta t$ and Δt denotes the time step. For each t_n, we thus need to solve the following boundary value problem:

$$\begin{cases}\beta G_0\mathbf{W}+(G_x\partial_x+G_y\partial_y+G_z\partial_z)\mathbf{W}=\mathbf{F}, \text{ in } \Omega,\\ (M_{\Gamma_m}-G_{\mathbf{n}})\mathbf{W}=0 \text{ on } \Gamma_m,\\ (M_{\Gamma_a}-G_{\mathbf{n}})\mathbf{W}=0 \text{ on } \Gamma_a.\end{cases} \tag{6}$$

where $\beta=\dfrac{2}{\Delta t}$, $\mathbf{W}=\mathbf{W}^{n+1}$ and $\mathbf{F}=\beta G_0\mathbf{W}^n-(G_x\partial_x+G_y\partial_y+G_z\partial_z)\mathbf{W}^n$. This system can be reformulated as a symmetric Friedrichs system and according to the results stated in [11], the associated boundary value problem (6) is well-posed in the functional space:

$$V=\{\mathbf{W}\in H(\text{curl})\times H(\text{curl}); (M_{\Gamma_m}-G_{\mathbf{n}})\mathbf{W}|_{\Gamma_m}=0,\ (M_{\Gamma_a}-G_{\mathbf{n}})\mathbf{W}|_{\Gamma_a}=0\}$$

The main motivation for using a Crank-Nicolson scheme rather than, for instance, a second order, upwind in time, implicit scheme is the following result concerning the conservation property of the semi-discrete electromagnetic energy.

Lemma 1 *Let a semi-discrete electromagnetic energy be defined by:*

$$\mathcal{E}^n=\frac{1}{2}\int_\Omega(\mathbf{W}^n)^t(G_0\mathbf{W}^n)dx=\frac{1}{2}\int_\Omega\varepsilon\parallel\mathbf{E}^n\parallel^2dx+\frac{1}{2}\int_\Omega\mu\parallel\mathbf{H}^n\parallel^2dx$$

then this energy is non-increasing in time, $\mathcal{E}^{n+1}\leq\mathcal{E}^n$, and it is exactly conserved in the absence of absorbing boundaries ($\Gamma_a=\emptyset$).

Proof if we take the scalar product of (5) by $\left(\dfrac{\mathbf{W}^{n+1}+\mathbf{W}^n}{2}\right)$ and integrate over Ω we obtain:

$$\frac{\mathcal{E}^{n+1}-\mathcal{E}^n}{\Delta t} = -\int_\Omega\left(\frac{\mathbf{W}^{n+1}+\mathbf{W}^n}{2}\right)^t\mathcal{G}_{xyz}\left(\frac{\mathbf{W}^{n+1}+\mathbf{W}^n}{2}\right)dx \tag{7}$$

with $\mathcal{G}_{xyz}\equiv(G_x\partial_x+G_y\partial_y+G_z\partial_z)$. We can easily see that:

$$\int_\Omega\mathbf{W}^t\mathcal{G}_{xyz}\mathbf{W}=\int_{\partial\Omega}\mathbf{W}^t(G_{\mathbf{n}}\mathbf{W})ds-\int_\Omega\mathbf{W}^t\mathcal{G}_{xyz}\mathbf{W}.$$

Therefore,

$$\begin{aligned}\int_\Omega \mathbf{W}^t \mathcal{G}_{xyz}\mathbf{W} &= \frac{1}{2}\int_{\partial\Omega} \mathbf{W}^t(G_{\mathbf{n}}\mathbf{W})ds,\\ &= \frac{1}{2}\int_{\Gamma_m} \mathbf{W}^t(G_{\mathbf{n}}\mathbf{W})ds + \frac{1}{2}\int_{\Gamma_a} \mathbf{W}^t(G_{\mathbf{n}}\mathbf{W})ds,\\ &= \frac{1}{2}\int_{\Gamma_m} \mathbf{W}^t(M_{\Gamma_m}\mathbf{W})ds + \frac{1}{2}\int_{\Gamma_a} \mathbf{W}^t(M_{\Gamma_a}\mathbf{W})ds,\end{aligned}$$

and using now the boundary operators (4) we get (since M_{Γ_m} is skew-symmetric and $|G_{\mathbf{n}}|$ is positive):

$$\int_\Omega \mathbf{W}^t(G_x\partial_x + G_y\partial_y + G_z\partial_z)\mathbf{W} = \frac{1}{2}\int_{\Gamma_a} \mathbf{W}^t(|G_{\mathbf{n}}|\mathbf{W})ds \geq 0. \tag{8}$$

From (7) and (8) the conclusion follows easily. ■

2.3 Semi-discretization in space

Let $\mathcal{T}_h$ be a discretisation of the computational Ω such that:

$$\overline{\Omega_h} \equiv \mathcal{T}_h = \bigcup_{K\in\mathcal{T}_h} \overline{K}$$

In this study, the numerical approximation $\mathbf{W}_h$ of the solution of problem (3) lies in the space $C^1([0,T];V_h)$ where:

$$V_h = \left\{\mathbf{V} \in [L^2(\Omega)]^3 \times [L^2(\Omega)]^3 |\ \forall K \in \mathcal{T}_h, Ve_{|K} \in \mathbb{P}_p(K)\right\}. \tag{9}$$

where $\mathbb{P}_p(K)$ denotes a space of polynomial elements of degree at most p over the element K.

By taking now the scalar product of (3) by a regular vector field $\mathbf{V}$ and integrating over an element K, we get:

$$\int_K (G_0\partial_t\mathbf{W}_h)^t\,\mathbf{V}dx + \int_K \left(\sum_{l\in\{x,y,z\}} G_l\partial_l\mathbf{W}_h\right)^t \mathbf{V}dx = 0 \quad , \quad \forall\mathbf{V}\in V_h, \tag{10}$$

and integration by parts yields:

$$\int_K (G_0 \partial_t \mathbf{W}_h)^t \mathbf{V} dx - \int_K \mathbf{W}_h^t \left(\sum_{l \in \{x,y,z\}} G_l \partial_l \mathbf{V} \right) dx + \int_{\partial K} (G_{\mathbf{n}_K} \mathbf{W}_h)^t \mathbf{V} ds = 0 \quad , \quad \forall \mathbf{V} \in V_h, \tag{11}$$

where $\mathbf{n}_K$ is the unit outward normal to the border of element K. In equation (11) we still need to define an approximation of the boundary integral operand, called *main numerical flux* in [11]-[12]. Then, Eq. (11) becomes:

$$\int_K (G_0 \partial_t \mathbf{W}_h)^t \mathbf{V} dx - \int_K \mathbf{W}_h^t \left(\sum_{l \in \{x,y,z\}} G_l \partial_l \mathbf{V} \right) dx + \sum_{F \in \partial K} \int_F (\Phi_F(\mathbf{W}_h))^t \mathbf{V} ds = 0 \quad , \quad \forall \mathbf{V} \in V_h. \tag{12a}$$

The definition of Φ_F needs to ensure the consistency of the approximation method. It depends on the type of face:

$$\Phi_F(\mathbf{W}_h) = \begin{cases} I_{F,K} G_{\mathbf{n}_F} \{\mathbf{W}_h\} \text{ if } F \in \mathcal{F}_0, \\ \frac{1}{2}(M_{F,K} + I_{F,K} G_{\mathbf{n}_F}) \mathbf{W}_h \text{ if } F \in \mathcal{F}_m, \\ \frac{1}{2}(M_{F,K} + I_{F,K} G_{\mathbf{n}_F}) \mathbf{W}_h \text{ if } F \in \mathcal{F}_a. \end{cases} \tag{12b}$$

where $\mathcal{F}_0$ denotes the set of purely internal faces of $\mathcal{T}_h$ and $\mathcal{F}_m$ (respectively $\mathcal{F}_a$) the set of faces on the boundary Γ_m (respectively Γ_a). Note that we adopt here a centered scheme as in [13], for the evaluation of the flux through an internal face $F \in \mathcal{F}_0$. Moreover, I denotes the *incidence matrix* between faces and elements of $\mathcal{T}_h$ whose dimension is $n_F \times n_E$ (n_F: number of faces and n_E: number of elements) and is defined by:

$$I_{F,K} = \begin{cases} 0 \text{ if } F \text{ does not belong to } K, \\ 1 \text{ if } F \in K \text{ and } F \text{ and } K \text{ have the same} \\ \quad \text{orientation (i.e } \text{sign}(\mathbf{n}_F^t \mathbf{n}_K) = 1), \\ -1 \text{ if } F \in K \text{ and } F \text{ and } K \text{ do not have} \\ \quad \text{the same orientation (i.e } (\text{sign}(\mathbf{n}_F^t \mathbf{n}_K) = -1). \end{cases}$$

For a face $F = K \cap \tilde{K}$ where $\tilde{K}$ is a neighboring element of K, we define the jump of the vector field $\mathbf{V}_h$ and its average as:

$$[\![\mathbf{V}_h]\!]_F = I_{F,K} \mathbf{V}_{h|K} + I_{F\tilde{K}} \mathbf{V}_{h|\tilde{K}} \quad \text{and} \quad \{\mathbf{V}_h\}_F = \frac{1}{2}(\mathbf{V}_{h|K} + \mathbf{V}_{h|\tilde{K}}). \tag{13}$$

where $\mathbf{V}_{h|K}$ denotes the restriction of $\mathbf{V}_h$ to the element K. In the present case, we use the centered flux for the internal faces [13] while for the faces F. For boundary faces, we set:

$$M_{F,K} = \begin{cases} I_{F,K} \begin{pmatrix} 0_{3\times 3} & N_{\mathbf{n}_F} \\ -N_{\mathbf{n}_F}^t & 0_{3\times 3} \end{pmatrix} \text{ if } F \in \mathcal{F}_m, \\ |G_{\mathbf{n}_F}| \text{ if } F \in \mathcal{F}_a. \end{cases} \tag{14}$$

Using now the weak form (12a) and by summing over all elements K of $\mathcal{T}_h$, the problem at hand is to find $\mathbf{W}_h \in V_h$ such that $\forall \mathbf{V} \in V_h$:

$$\begin{aligned} \int_{\Omega_h} \left(G_0 \partial_t \mathbf{W}_h\right)^t \mathbf{V} dx - \sum_{K\in\mathcal{T}_h} \int_K \mathbf{W}_h^t \left(\sum_{l\in\{x,y,z\}} G_l \partial_l \mathbf{V} \right) dx \\ + \sum_{F\in\mathcal{F}_m\cup\mathcal{F}_a} \int_F \left(\frac{1}{2} (M_{F,K} + I_{F,K} G_{\mathbf{n}_F}) \mathbf{W}_h \right)^t \mathbf{V} ds \\ + \sum_{F\in\mathcal{F}_0} \int_F \left(G_{\mathbf{n}_F} \{\mathbf{W}_h\}_F\right)^t [\![\mathbf{V}]\!]_F ds = 0. \end{aligned} \tag{15}$$

This weak formulation is inspired by [11, equation (4.26)] and adapted to problem (3). The convergence properties of the semi-discretized problem have been studied in [13] where its is shown that the spatial error behaves as $\mathcal{O}(h^{\min(p,s)})$ where p is the polynomial order and s comes from the assumed regularity of the solution of the continuous problem.

2.4 Properties of the totally discretized problem

First remark that the last integral term of Eq.(15) can be rewritten as (with $\tilde{K}$ a neighboring element of K) :

$$\begin{aligned} \sum_{F\in\mathcal{F}_0} \int_F \left(G_{\mathbf{n}_F} \{\mathbf{W}_h\}_F\right)^t [\![\mathbf{V}]\!]_F ds &= \sum_{K\in\mathcal{T}_h} \sum_{\substack{F\in\partial K \\ F\in\mathcal{F}_0}} \int_F \frac{1}{2} \left(G_{\mathbf{n}_F} \mathbf{W}_{h|K}\right)^t \left(I_{F,K} \mathbf{V}_{|K}\right) ds \\ &+ \sum_{K\in\mathcal{T}_h} \sum_{\substack{F\in\partial K \\ F\in\mathcal{F}_0}} \int_F \frac{1}{2} \left(G_{\mathbf{n}_F} \mathbf{W}_{h|\tilde{K}}\right)^t \left(I_{F,K} \mathbf{V}_{|K}\right) ds, \end{aligned}$$

thus:

$$\begin{aligned}\sum_{F\in\mathcal{F}_0}\int_F \left(G_{\mathbf{n}_F}\{\mathbf{W}_h\}_F\right)^t [\![\mathbf{V}]\!]_F &+ \sum_{F\in\mathcal{F}_m\cup\mathcal{F}_a}\int_F \left(\frac{1}{2}(M_{F,K}+I_{F,K}G_{\mathbf{n}_F})\mathbf{W}_h\right)^t \mathbf{V}ds \\ &= \sum_{K\in\mathcal{T}_h}\int_{\partial K}\frac{1}{2}\left(G_{\mathbf{n}_F}\mathbf{W}_{h|K}\right)^t\left(I_{F,K}\mathbf{V}_{|K}\right)ds \\ &+ \sum_{K\in\mathcal{T}_h}\sum_{\substack{F\in\partial K\\ F\in\mathcal{F}_0}}\int_F\frac{1}{2}\left(G_{\mathbf{n}_F}\mathbf{W}_{h|\tilde{K}}\right)^t\left(I_{F,K}\mathbf{V}_{|K}\right)ds \\ &+ \sum_{K\in\mathcal{T}_h}\sum_{\substack{F\in\partial K\\ F\in(\mathcal{F}_m\cup\mathcal{F}_a)}}\int_F\frac{1}{2}\left(M_{F,K}\mathbf{W}_{h|K}\right)^t\mathbf{V}_{|K}ds,\end{aligned}$$

but:

$$\begin{aligned}\int_{\partial K}\left(G_{\mathbf{n}_F}\mathbf{W}_{h|K}\right)^t\left(I_{F,K}\mathbf{V}_{|K}\right)ds &= \int_K \mathbf{W}_h^t\left(\sum_{l\in\{x,y,z\}}G_l\partial_l\mathbf{V}\right)dx \\ &+ \int_K\left(\sum_{l\in\{x,y,z\}}G_l\partial_l\mathbf{W}_h\right)^t\mathbf{V}dx,\end{aligned}$$

Taking into account the above expressions, Eq.(15) becomes:

$$\begin{aligned}\int_{\Omega_h}(G_0\partial_t\mathbf{W}_h)^t\mathbf{V}dx &- \frac{1}{2}\sum_{K\in\mathcal{T}_h}\int_K\mathbf{W}_h^t\left(\sum_{l\in\{x,y,z\}}G_l\partial_l\mathbf{V}\right)dx \\ &+ \frac{1}{2}\int_K\left(\sum_{l\in\{x,y,z\}}G_l\partial_l\mathbf{W}_h\right)^t\mathbf{V}dx \\ &+ \frac{1}{2}\sum_{K\in\mathcal{T}_h}\sum_{\substack{F\in\partial K\\ F\in\mathcal{F}_0}}\int_F\left(G_{\mathbf{n}_F}\mathbf{W}_{h|\tilde{K}}\right)^t\left(I_{F,K}\mathbf{V}_{|K}\right)ds \\ &+ \frac{1}{2}\sum_{K\in\mathcal{T}_h}\sum_{\substack{F\in\partial K\\ F\in(\mathcal{F}_m\cup\mathcal{F}_a)}}\int_F\left(M_{F,K}\mathbf{W}_{h|K}\right)^t\mathbf{V}_{|K}ds=0,\end{aligned}$$

or equivalently:

$$\begin{array}{l} 2\displaystyle\int_{\Omega_h} \left(G_0 \partial_t \mathbf{W}_h\right)^t \mathbf{V} dx - \sum_{K\in\mathcal{T}_h} \int_K \mathbf{W}_h^t \left(\sum_{l\in\{x,y,z\}} G_l \partial_l \mathbf{V} \right) dx + \\ \displaystyle\sum_{K\in\mathcal{T}_h} \int_K \left(\sum_{l\in\{x,y,z\}} G_l \partial_l \mathbf{W}_h \right)^t \mathbf{V} dx + \\ \displaystyle\sum_{F\in\mathcal{F}_0} \int_F \left[\left(G_{\mathbf{n}_F} \mathbf{W}_{h|K}\right)^t \left(I_{F,\tilde{K}} \mathbf{V}_{|\tilde{K}}\right) + \left(G_{\mathbf{n}_F} \mathbf{W}_{h|\tilde{K}}\right)^t \left(I_{F,K} \mathbf{V}_{|K}\right) \right] ds + \\ \displaystyle\sum_{F\in\mathcal{F}_m\cup\mathcal{F}_a} \int_F \left(M_{F,K} \mathbf{W}_h\right)^t \mathbf{V} ds = 0. \end{array} \tag{16}$$

We now introduce the following bilinear forms:

$$\left\{ \begin{array}{rcl} a(\mathbf{W},\mathbf{V}) & = & 2\displaystyle\int_{\Omega_h} \left(G_0 \mathbf{W}\right)^t \mathbf{V} dx, \\ b(\mathbf{W},\mathbf{V}) & = & \displaystyle -\int_{\Omega_h} \mathbf{W}^t \left(\sum_{l\in\{x,y,z\}} G_l \partial_l \mathbf{V} \right) dx + \int_{\Omega_h} \left(\sum_{l\in\{x,y,z\}} G_l \partial_l \mathbf{W} \right)^t \mathbf{V} dx, \\ c(\mathbf{W},\mathbf{V}) & = & \displaystyle\sum_{F\in\mathcal{F}_0} \int_F \left[\left(G_{\mathbf{n}_F} \mathbf{W}_{|K}\right)^t \left(I_{F,\tilde{K}} \mathbf{V}_{|\tilde{K}}\right) + \left(G_{\mathbf{n}_F} \mathbf{W}_{|\tilde{K}}\right)^t \left(I_{F,K} \mathbf{V}_{|K}\right) \right] ds \\ & + & \displaystyle\sum_{F\in\mathcal{F}_m\cup\mathcal{F}_a} \int_F \left(M_{F,K} \mathbf{W}\right)^t \mathbf{V} ds \end{array} \right.$$

Thus (15) is equivalent to find $\mathbf{W}_h \in V_h$ such that $\forall \mathbf{V} \in V_h$:

$$a(\partial_t \mathbf{W}, \mathbf{V}) + b(\mathbf{W}, \mathbf{V}) + c(\mathbf{W}, \mathbf{V}) = 0,\ \forall \mathbf{V} \in V_h. \tag{17}$$

Note that the bilinear form $b(\mathbf{W},\mathbf{V})$ is skew-symmetric thus $b(\mathbf{W}_h,\mathbf{W}_h) = 0$. Furthermore, since $G_{\mathbf{n}_F}$ is symmetric and $I_{F,\tilde{K}} = -I_{F,K}$ we obtain:

$$c(\mathbf{W}_h,\mathbf{W}_h) = \sum_{F\in\mathcal{F}_m\cup\mathcal{F}_a} \int_F \left(M_{F,K} \mathbf{W}_h\right)^t \mathbf{W}_h ds.$$

and, using the boundary operators (4) and since M_{Γ_m} is skew-symmetric:

$$c(\mathbf{W}_h,\mathbf{W}_h) = \sum_{F\in\mathcal{F}_a} \int_F \left(|G_{\mathbf{n}_F}| \mathbf{W}_h\right)^t \mathbf{W}_h ds. \tag{18}$$

The totally discretized problem by the Crank-Nicolson scheme is then to find $\mathbf{W}_h^{n+1} \in V_h$ such that $\forall \mathbf{V} \in V_h$:

$$\begin{aligned} \beta a(\mathbf{W}_h^{n+1}, \mathbf{V}) &+ b(\mathbf{W}_h^{n+1}, \mathbf{V}) + c(\mathbf{W}_h^{n+1}, \mathbf{V}) \\ &= \beta a(\mathbf{W}_h^{n}, \mathbf{V}) - b(\mathbf{W}_h^{n}, \mathbf{V}) - c(\mathbf{W}_h^{n}, \mathbf{V}), \end{aligned} \tag{19}$$

where $\beta = \dfrac{2}{\Delta t}$, given $W_h^0 = W_h(0)$, where $W_h(0)$ is the discretization of the intial condition. This discrete problem has a unique solution as stated by the following result.

Lemma 2 *The homogeneous discrete problem*

$$\begin{gathered} \textit{Find } \mathbf{W}_h \in V_h \textit{ such that} \\ \beta a(\mathbf{W}_h, \mathbf{V}) + b(\mathbf{W}_h, \mathbf{V}) + c(\mathbf{W}_h, \mathbf{V}) = 0, \, \forall \mathbf{V} \in V_h. \end{gathered} \tag{20}$$

possesses only the trivial solution.

Proof Using Eq. (18) and the fact that the bilinear form $b(\mathbf{W}, \mathbf{V})$ is skew-symmetric we get:

$$\begin{aligned} \beta a(\mathbf{W}_h, \mathbf{W}_h) + b(\mathbf{W}_h, \mathbf{W}_h) + c(\mathbf{W}_h, \mathbf{W}_h) &= 2\beta \int_{\Omega_h} \left(G_0 \mathbf{W}_h\right)^t \mathbf{W}_h dx \\ &+ \sum_{F \in \mathcal{F}_a} \int_F \mathbf{W}_h^t |G_{\mathbf{n}_F}| \mathbf{W}_h ds = 0. \end{aligned}$$

Since G_0 is symmetric positive definite and $|G_{\mathbf{n}_F}|$ is positive, the conclusion follows. ■

A direct consequence of the fact that the bilinear form $b(\mathbf{W}, \mathbf{V})$ is skew-symmetric and of property (18) is the following discrete counterpart of Lemma 1.

Lemma 3 *If we define the discrete energy by:*

$$\mathcal{E}_h^n = \frac{1}{4} a(\mathbf{W}_h^n, \mathbf{W}_h^n), \tag{21}$$

then this energy is non-increasing in time, $\mathcal{E}_h^{n+1} \leq \mathcal{E}_h^n$, and it is exactly conserved in absence of absorbing boundaries ($\Gamma_a = \emptyset$).

Proof Choose as a test function $\mathbf{V} = \dfrac{\mathbf{W}_h^{n+1} + \mathbf{W}_h^n}{2}$ in (19) and use the the facts that $b(\mathbf{W}, \mathbf{V})$ is a skew-symmetric bilinear form, and that $G_{\mathbf{n}_F}$ and $|G_{\mathbf{n}_F}|$ are symmetric matrices. ■

In summary, the totally discretized problem, which can be seen as a time discretization of a system of ordinary differential equations, is unconditionally stable and second order accurate in time. The spatial accuracy is given by the convergence properties of the discontinuous Galerkin method using centered fluxes [13]. Finally, it preserves a discrete electromagnetic energy, which is an important property for long time simulations.

3 Numerical results

3.1 Two-dimensional Maxwell equations

The proposed implicit DGTD method has been first applied to the numerical resolution of the two-dimensional transverse magnetic Maxwell equations:

$$\begin{cases} \mu \dfrac{\partial H_x}{\partial t} + \dfrac{\partial E_z}{\partial y} = 0, \\ \mu \dfrac{\partial H_y}{\partial t} - \dfrac{\partial E_z}{\partial x} = 0, \\ \varepsilon \dfrac{\partial E_z}{\partial t} - \dfrac{\partial H_y}{\partial x} + \dfrac{\partial H_x}{\partial y} = 0. \end{cases}$$

The implicit DGTD method proposed here requires the resolution of a sparse linear system at each time step however, for non-dispersive materials, the coefficient of this system are time independent, a feature that can be taken into account to minimize the additional computational overhead. Consequently, in this study, we decided to use a LU factorization method for sparse matrices more precisely, the MUMPS multifrontal sparse matrix solver [4]. The sparse matrix characterizing the implicit DGTD method has a block structure where the size of a block is $3n_p \times 3n_p$, n_p being the number of degrees of freedom associated to a nodal polynomial basis of the space $\mathbb{P}_p$ i.e $n_p = ((p+1)(p+2))/2$. This matrix is factored once for all before the time stepping loop. Then, each linear system inversion amounts to a forward and a backward solve using the triangular L and U factors.

3.2 Eigenmode in a metallic cavity

The first test case that we consider is the propagation of an eigenmode in a unitary square cavity with perfectly conducting walls. This test case allows a direct comparison with an exact solution. Here, it will also be used to demonstrate that we cannot take advantage of the proposed implicit DGTD-$\mathbb{P}_p$ method if the underlying mesh is uniform (or quasi-uniform) while substantial reductions of the computing time can be achieved in the case of a non-uniform mesh. For this purpose, we make use of two triangular meshes (see Fig. 1):

- a uniform mesh consisting of 1681 vertices and 3200 triangles. The non-dimensioned time step corresponding to CFL-$\mathbb{P}_0$=1 is $(\Delta t)_u = 0.017678$ m (the physical time step is defined by $\overline{(\Delta t)_u} = (\Delta t)_u/3.10^8$ s). For the interpolation orders $p \geq 1$, the time step actually used is CFL-$\mathbb{P}_p \times (\Delta t)_u$ where CFL-$\mathbb{P}_p$ is the CFL number associated to the DGTD-$\mathbb{P}_p$ method.

- a non-uniform mesh consisting of 1400 vertices and 2742 triangles. The ratio between the largest and smallest edges of this mesh is 178. In this case, the minimum and maximum values of the time step are respectively given by $(\Delta t)_m = 0.000434$ m and $(\Delta t)_M = 0.070617$ m. The time step used in the simulations is CFL-$\mathbb{P}_p \times (\Delta t)_m$.

For the explicit DGTD-$\mathbb{P}_p$ method, CFL-$\mathbb{P}_p \leq 1$ and the actual value is dictated by stability issues while CFL-$\mathbb{P}_p$ can be set to an arbitrarily large value for the implicit DGTD-$\mathbb{P}_p$ method but is constrained in practice by accuracy issues as it will be shown in the sequel. Results are given on Fig. 2 to 6 in the form of the time evolution of various quantities: the L2 error between the numerical and exact solutions, the discrete energy (21) and the E_z component of the electric field. The simulations were carried out for ten periods. Computing times are summarized in Tab. 1 and 2. It is clear from these results that a second order implicit time integration scheme is not a good option if the underlying mesh is uniform. Indeed, the numerical dispersion introduced by the Crank-Nicolson scheme notably degrades the overall accuracy of the calculation. However, if a non-uniform mesh is used then an implicit scheme becomes a viable strategy despite the computational overhead of the solution of a linear system at each time iteration. Taking into account the time behavior of the L2 error on Fig. 4 and 5, we see that a CFL value of 12.0 (respectively 4.0) for the implicit DGTD-$\mathbb{P}_1$ method (respectively DGTD-$\mathbb{P}_2$ method) yields an acceptable solution. For these values of the CFL, the gain in overall computing (CPU) times between the implicit and explicit methods is respectively equal to 3.3 and 2.2 (note that the given CPU times include the factorization times).

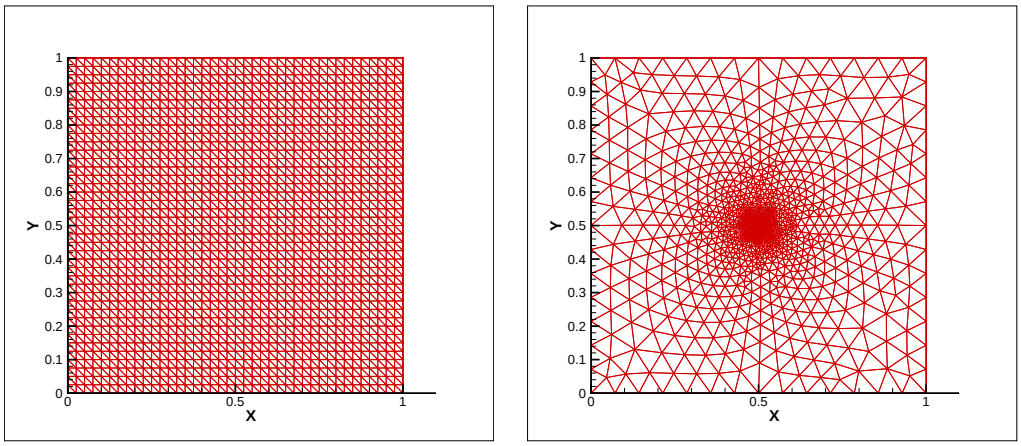

Figure 1: Uniform (left) and non-uniform (right) meshes of a unitary square cavity

3.3 Diffraction of a plane wave by a square

The second test case that we consider is the diffraction of a plane wave by a perfectly conducting square of side length c = 0.25 m. The far-field boundary Γ_a where the first order Silver-Müler absorbing condition is applied is defined as a square of side length c = 1.0 m. Both squares are centered at the origin [0.0 , 0.0]. We make use of a non-uniform mesh (see Fig. 7) consisting of 6018 vertices and 10792 triangles. The ratio between the largest

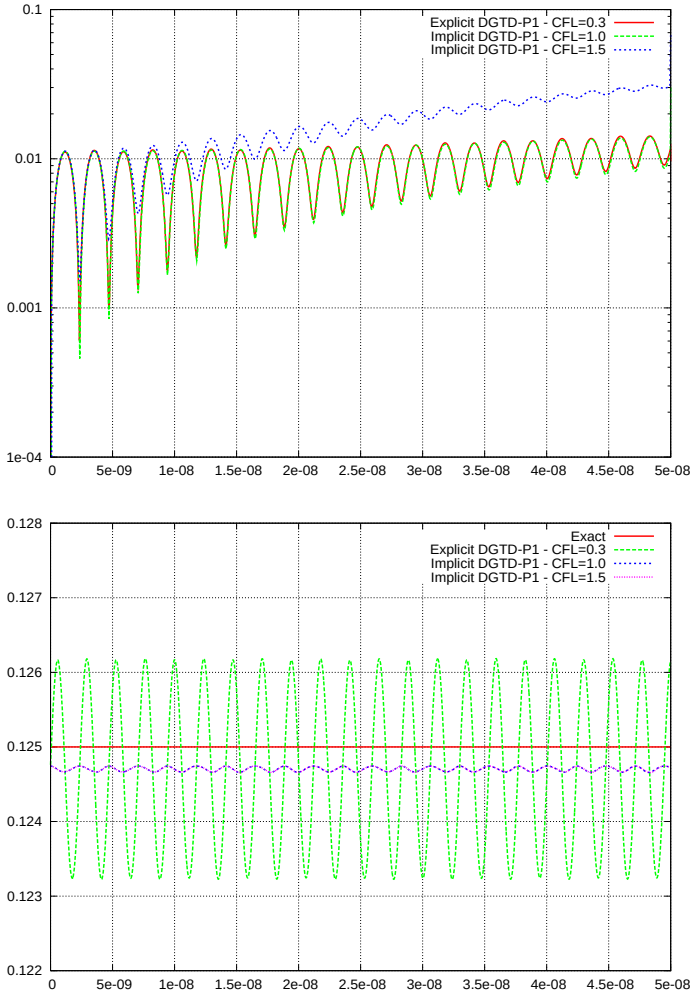

Figure 2: Eigenmode in a unitary square cavity - Uniform mesh
DGTD-$\mathbb{P}_1$ method: time evolutions of the L2 error (top) and discrete energy (bottom)

Time integration	Method	CFL-$\mathbb{P}_p$	CPU time
Explicit	DGTD-$\mathbb{P}_1$	0.3	15 sec
Implicit	-	1.0	44 sec
-	-	1.5	30 sec

Table 1: Eigenmode in a unitary square cavity - Uniform mesh
CPU times (AMD Opteron 2 GHz based workstation)

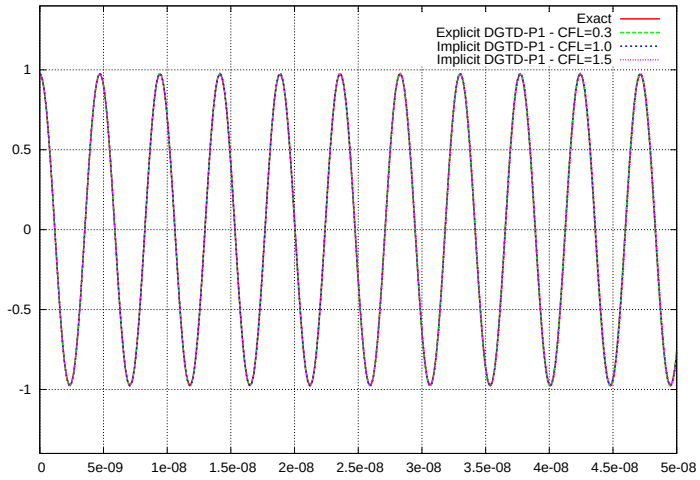

Figure 3: Eigenmode in a unitary square cavity - Uniform mesh
Time evolution of E_z: DGTD-$\mathbb{P}_1$ method

Time integration	Method	CFL-$\mathbb{P}_p$	CPU time
Explicit	DGTD-$\mathbb{P}_1$	0.3	443 sec
Implicit	-	12.0	133 sec
-	-	24.0	67 sec
Explicit	DGTD-$\mathbb{P}_2$	0.2	2057 sec
Implicit	-	2.0	1923 sec
-	-	4.0	938 sec
-	-	6.0	620 sec

Table 2: Eigenmode in a unitary square cavity - Non-uniform mesh
CPU times (AMD Opteron 2 GHz based workstation)

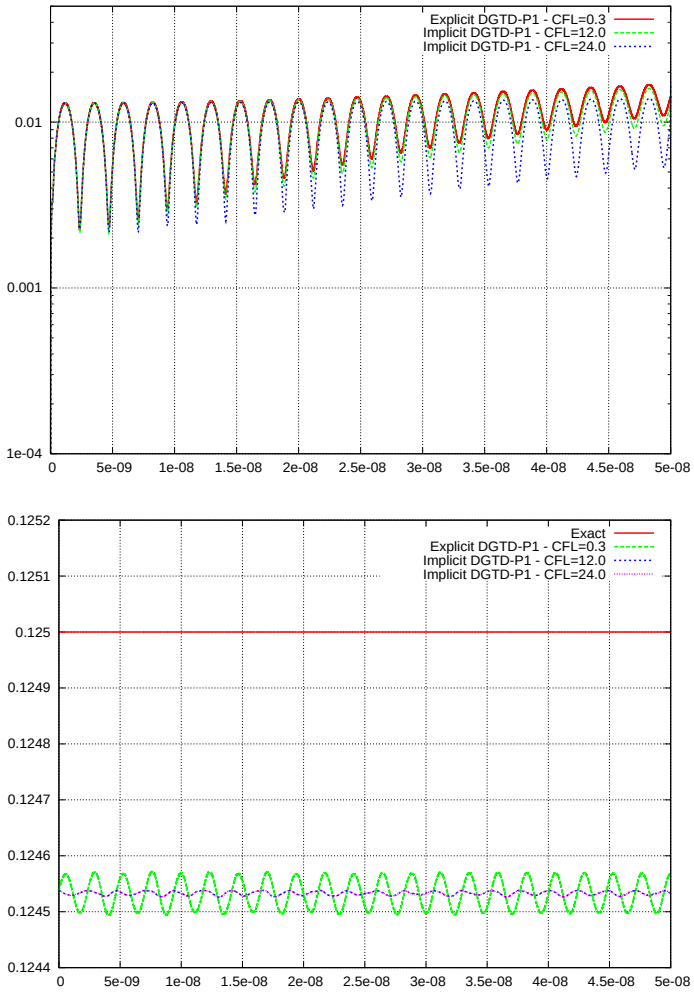

Figure 4: Eigenmode in a unitary square cavity - Non-uniform mesh
DGTD-$\mathbb{P}_1$ method: time evolutions of the L2 error (top) and discrete energy (bottom)

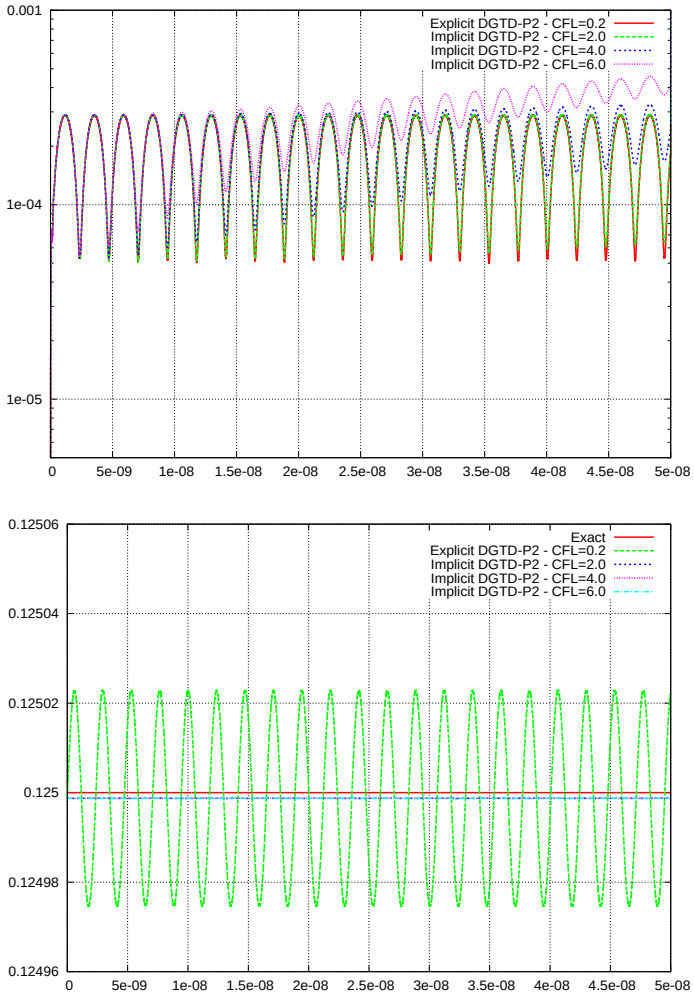

Figure 5: Eigenmode in a unitary square cavity - Non-uniform mesh
DGTD-$\mathbb{P}_2$ method: time evolutions of the L2 error (top) and discrete energy (bottom)

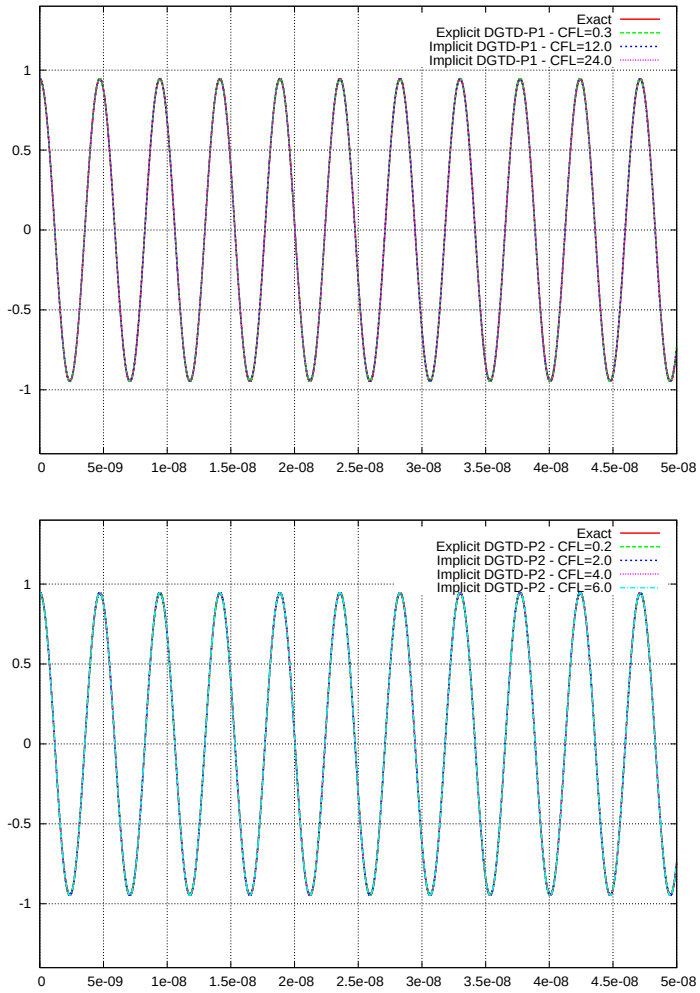

Figure 6: Eigenmode in a unitary square cavity - Non-uniform mesh
Time evolution of E_z: DGTD-$\mathbb{P}_1$ method (top) and DGTD-$\mathbb{P}_2$ method (bottom)

and smallest edges of this mesh is 357. In this case, the minimum and maximum values of the time step are respectively given by $(\Delta t)_m = 0.000286$ m and $(\Delta t)_M = 0.098589$ m. As previously, the time step used in the simulations is CFL-$\mathbb{P}_p \times (\Delta t)_m$. Simulations have been conducted for three frequencies of the incident plane wave, F=300 MHz, F=600 MHz and F=900 MHz. In each case, simulations are carried out for then periods and a discrete Fourier transform is applied to the field components during the last period.

Results are shown on Fig. 8 to 10 in terms of the x-wise 1D distribution for $y = 0.25$ m of the discrete Fourier transform (DFT) of E_z. For each configuration (DGTD-$\mathbb{P}_p$ method and frequency F), we show the distribution of DFT(E_z) for the time explicit calculation which is considered here as the reference solution, and two distributions of DFT(E_z) corresponding to time implicit calculations using respectively the maximum allowable CFL yielding a solution that fit the reference one, and a larger CFL yielding a less accurate solution. Note that these 1D distributions are plotted in terms of the degrees of freedom that are located on the line $y = 0.25$ m (see also Fig. 7) and the associated values of DFT(E_z) are computed as the mean value of the local, element-wise, values. Computing times are summarized in Tab. 3. These results call for two main remarks:

- as expected, the maximum allowable CFL value decreases when the frequency of the incident plane wave increases. Not surprisingly, despite the fact that the implicit DGTD method is unconditionally stable, the maximum allowable CFL value is generally dictated by physical considerations.

- as a result, for a given interpolation order, the gain in CPU time i.e the ratio of CPU time of the explicit DGTD calculation to the CPU time of the implicit DGTD calculation, decreases when the frequency increases. For instance, for $p = 2$ this ratio ranges from 7.5 for F=300 MHz to 3.0 for F=900 MHz. However, for a given frequency, this gain increases with the interpolation order: for F=900 MHz, this ratio is respectively equal to 3.0 for $p = 2$ and 5.5 for $p = 3$.

4 Conclusion and future works

In this paper we have studied an implicit DGTD-$\mathbb{P}_p$ method for solving the time domain Maxwell equations on unstructured triangular meshes. This method is non-dissipative, second order accurate in time an $p+1$-th order accurate in space. As usual with time implicit schemes, this method requires the resolution of a sparse linear system at each time step. For non-dispersive materials, the coefficients of the associated sparse matrix are constant in time. Taking into account this feature in the linear system solution strategy is a key ingredient for obtaining a computationally efficient method. For two-dimensional problems, a direct solver based on a LU factorization such as the one adopted in this study is generally considered as the optimal strategy, at least from the computing time point of view. In this study, by adopting a multifrontal sparse matrix solver, we have clearly demonstrated that

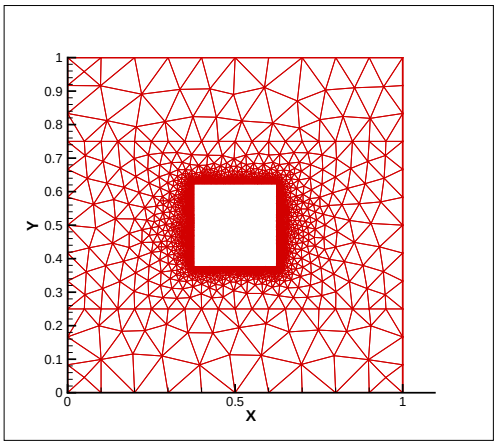

Figure 7: Diffraction of a plane wave by a square: triangular mesh

Frequency	Time integration	Method	CFL-$\mathbb{P}_p$	CPU time
300 MHz	Explicit	DGTD-$\mathbb{P}_1$	0.3	1602 sec
-	Implicit	-	15.0	370 sec
-	Explicit	DGTD-$\mathbb{P}_2$	0.2	5677 sec
-	Implicit	-	15.0	762 sec
600 MHz	Explicit	DGTD-$\mathbb{P}_1$	0.3	758 sec
-	Implicit	-	7.0	383 sec
-	Explicit	DGTD-$\mathbb{P}_2$	0.2	3074 sec
-	Implicit	-	7.0	767 sec
900 MHz	Explicit	DGTD-$\mathbb{P}_2$	0.2	2191 sec
-	Implicit	-	5.0	746 sec
-	Explicit	DGTD-$\mathbb{P}_3$	0.1	8771 sec
-	Implicit	-	5.0	1591 sec

Table 3: Diffraction of a plane wave by a square
CPU times (AMD Opteron 2 GHz based workstation)

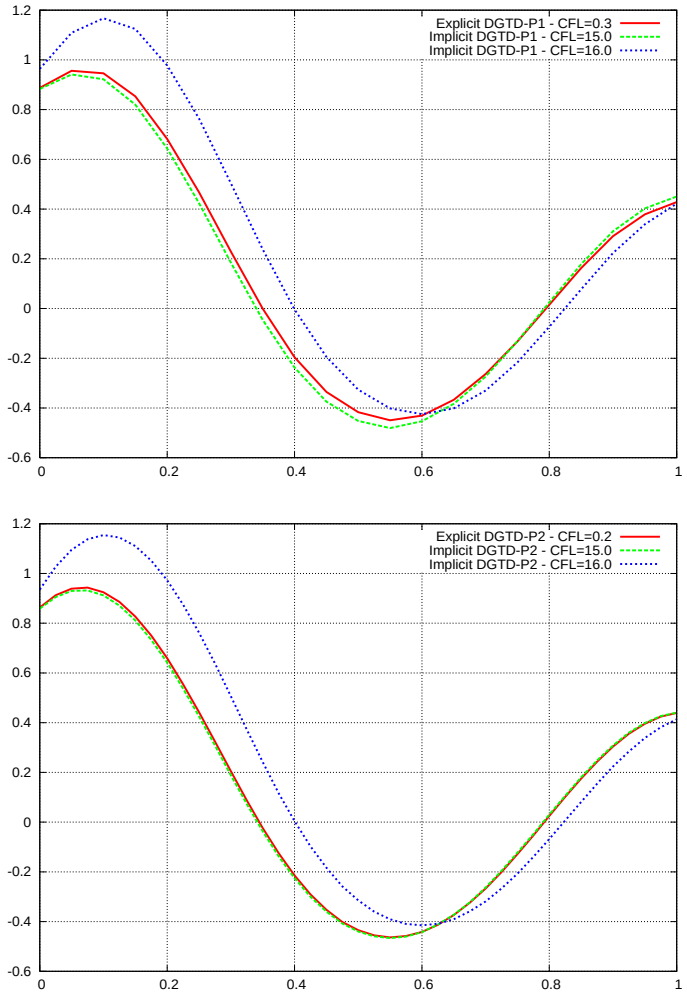

Figure 8: Diffraction of a plane wave by a square: F=300 MHz
1D distribution of DFT(E_z), $y = 0.75$ m
Top: DGTD-$\mathbb{P}_1$ method - Bottom: DGTD-$\mathbb{P}_2$ method

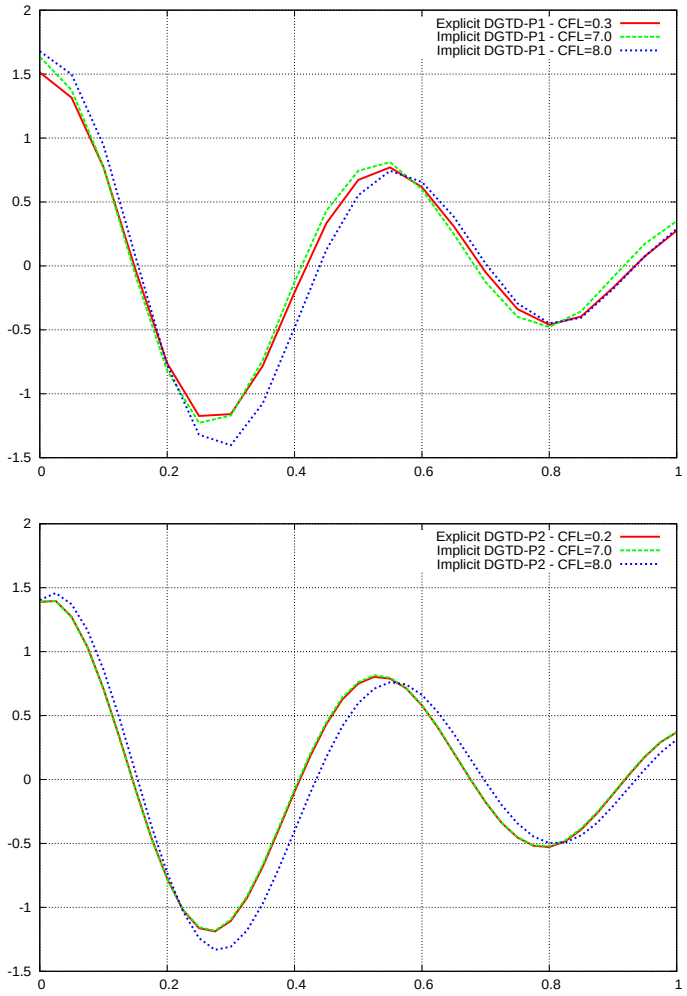

Figure 9: Diffraction of a plane wave by a square: F=600 MHz
1D distribution of DFT(E_z), $y = 0.75$ m
Top: DGTD-$\mathbb{P}_1$ method - Bottom: DGTD-$\mathbb{P}_2$ method

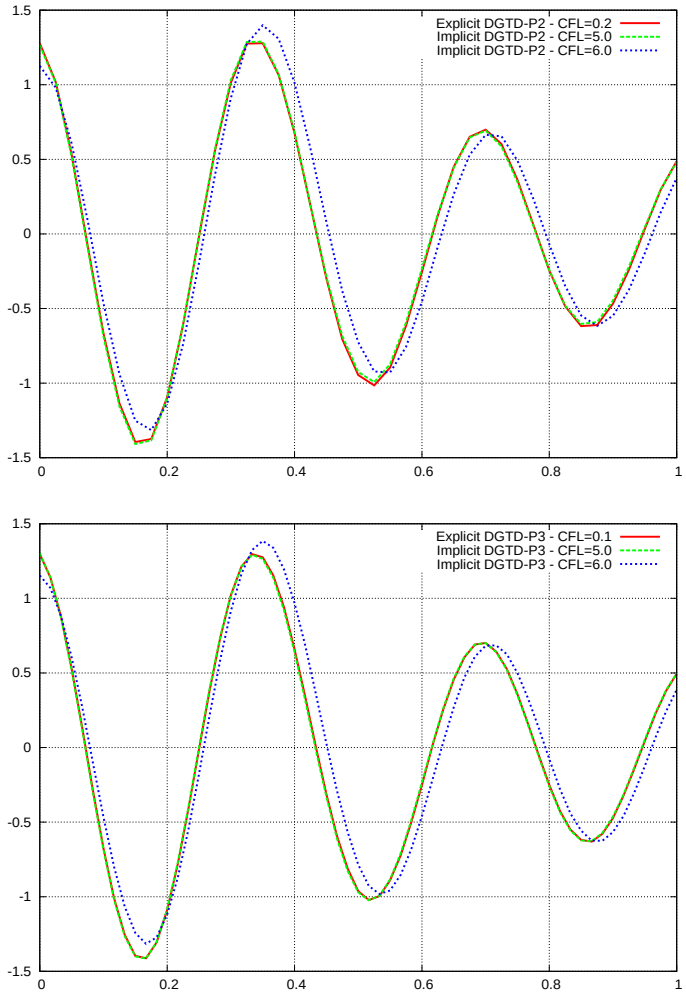

Figure 10: Diffraction of a plane wave by a square: F=900 MHz
1D distribution of DFT(E_z), $y = 0.75$ m
Top: DGTD-$\mathbb{P}_2$ method - Bottom: DGTD-$\mathbb{P}_3$ method

an implicit discontinuous Galerkin time domain is a viable numerical strategy for solving electromagnetic wave propagation problems on locally refined unstructured meshes.

Concerning future works, our first objective will be to adapt the implicit DGTD-$\mathbb{P}_p$ method proposed here to the case of the three-dimensional time domain Maxwell equations. From the mathematical formulation point of view, this extension will be straightforward. Moreover, we can reasonably expect that the theoretical results of section 2 will still be valid in the 3D case. However, from the computational efficiency viewpoint, it is clear that a global direct direct solver such as the multifrontal method adopted in this study will not be an acceptable option due to the large memory capacity required for the simulation of realistic three-dimensional problems, especially if the computational domain is discretized using unstructured tetrahedral meshes. In this context, parallel computing will be a mandatory path and although MUMPS [4] is a parallel sparse matrix solver, we plan to consider a Schwarz type domain decomposition method [10] as a mean to build an hybrid iterative/direct solver, and still benefit from the fact that the sparse matrix associated to a sub-domain problem can be factored once for all before the time stepping loop.

On the other hand, a characteristic of our implicit DGTD-$\mathbb{P}_p$ method which can be improved is the time accuracy through the choice of an alternative implicit time integration scheme. Indeed, the Crank-Nicolson scheme used in this study is non-dissipative and second-order accurate. However, it is also characterized by a second order numerical dispersion which is the main factor limiting the CFL that can be used in practice. One possible approach to increase the accuracy of the Crank-Nicolson scheme is to apply a defect-correction in time procedure [16]. An expected advantage of this accuracy enhancement strategy is that it will preserve basic properties of the underlying second order accurate scheme among which, unconditional stability.

Finally, one may question about the viability of a globally implicit time integration strategy in certain practical situations such as those involving a triangulation which is uniform almost everywhere except in a localized region where the mesh is highly refined and unstructured. In such cases, a locally implicit strategy [22] will probably prove to be the most appropriate strategy. Designing such a locally implicit (or hybrid explicit/implicit) DGTD-$\mathbb{P}_p$ will be considered in a future work.

References

[1] *Discontinuous Galerkin methods. Theory, computation and applications*, Lecture Notes in Computational Science and Engineering, **11**, B. Cockburn, G.E. Karniadakis and C.W. Shu Eds., Springer-Verlag (2000).

[2] *Special issue on discontinuous Galerkin method*, J. Sci. Comput., **22-23**, B. Cockburn and C.W. Shu Eds., Springer (2005).

[3] *Special issue on discontinuous Galerkin method*, Comput. Meth. App. Mech. Engng., **195**, C. Dawson Ed., Elsevier (2006).

[4] P.R. Amestoy, I.S. Duff and J.-Y. L'Excellent, *Multifrontal parallel distributed symmetric and unsymmetric solvers*, Comput. Meth. App. Mech. Engng., **184**, 501-520 (2000).

[5] M. Bernacki, L. Fezoui, S. Lanteri and S. Piperno, *Parallel unstructured mesh solvers for heterogeneous wave propagation problems*, Appl. Math. Model., **30 (8)**, 744-763 (2006).

[6] S. Chaillou, J. Wiart and W. Tabbara, *A subgridding scheme based on mesh nesting for the FDTD method*, Microwave and Optical Technology Letters, **22 (3)**, 211-214 (1999).

[7] M.-H. Chen, B. Cockburn and Fernando Reitich, *High-order RKDG methods for computational electromagnetics*, J. Sci. Comput., **22-23**, 205-226 (2005).

[8] J.-P. Cioni, L. Fezoui and H. Steve, *A parallel time-domain Maxwell solver using upwind schemes and triangular meshes*, IMPACT Comput. Sci. Eng., **5 (3)**, 215-247 (1993)

[9] B. Cockburn, F. Li and Chi-Wang Shu, *Locally divergence-free discontinuous Galerkin methods for the Maxwell equations*, J. Comput. Phys., **194 (2)**, 588-610 (2004).

[10] V. Dolean, L. Gerardo-Giorda and M. Gander, *Optimized Schwarz methods for Maxwell equations*, submitted (2006). Also available as a preprint at the URL https://hal.archives-ouvertes.fr/ccsd-00107263.

[11] A. Ern and J.L. Guermond, *Discontinuous Galerkin methods for Friedrichs' systems. I. General theory*, SIAM J. Numer. Anal., **44 (2)**, 753-778 (2006).

[12] A. Ern and J.L. Guermond, *Discontinuous Galerkin methods for Friedrichs' systems. II. Second-order elliptic PDE's*, SIAM J. Numer. Anal., **44 (6)**, 2363-2388 (2006).

[13] L. Fezoui, S. Lanteri, S. Lohrengel and S. Piperno, *Convergence and stability of a discontinuous Galerkin time-domain method for the 3D heterogeneous Maxwell equations on unstructured meshes*, RAIRO Modél. Math. Anal. Numér., **39 (6)**, 1149-1176 (2005).

[14] S.G. Garcia and T.W. Lee and S.C. Hagness *On the accuracy of the ADI-FDTD method*, IEEE Trans. Antennas and Wir. Propag. Lett., **1**, 31-34 (2002).

[15] J. S. Hesthaven and T. Warburton, *Nodal high-order methods on unstructured grids. I. Time-domain solution of Maxwell's equations*, J. Comput. Phys., **181 (1)**, 186-221 (2002).

[16] J. Lee and B. Fornberg, *Some unconditionally stable time stepping methods for the 3-D Maxwell's equations*, J. Comput. Appl. Math., **166**, 497-523 (2004).

[17] P. Monk and G.R. Richter, *A discontinuous Galerkin method for linear symmetric hyperbolic systems in inhomogeneous media*, J. Sci. Comput., **22-23**, 443-477 (2005).

[18] T. Namiki, *3-D ADI-FDTD method unconditionally stable time-domain algorithm for solving full vector Maxwell's equations*, IEEE Trans. Microwave Theory Tech., **48 (10)**, 1743-1748 (2000).

[19] D.W. Peaceman and H.H. Rachford, *The numerical solution of parabolic and elliptic differential equations*, J. Soc. Indust. Appl. Math., **3** 28-41 (1955).

[20] S. Pernet, X. Ferrieres and G. Cohen, *High spatial order finite element method to solve Maxwell's equations in time domain*, IEEE Trans. Antennas and Propag., **53 (9)**, 2889-2899 (2005).

[21] G. Cohen, X. Ferrieres and S. Pernet, *A spatial high spatial order hexahedral discontinuous Galerkin method to solve Maxwell's equations in time domain*, J. Comput. Phys., **217 (2)**, 340-363 (2006).

[22] S. Piperno, *Symplectic local time-stepping in non-dissipative DGTD methods applied to wave propagation problem*, ESAIM: Math. Model. Num. Anal., to appear (2007).

[23] K.S. Yee, *Numerical solution of initial boundary value problems involving Maxwell's equations in isotropic media*, IEEE Trans. Antennas and Propag., **14 (3)**, 302-307 (1966).

[24] F. Zheng and Z. Chen, *Numerical dispersion analysis of the unconditionally stable 3-D ADI-FDTD method*, IEEE Trans. Microwave Theory Tech., **49 (5)**, 1006-1009 (2001).

Unité de recherche INRIA Sophia Antipolis
2004, route des Lucioles - BP 93 - 06902 Sophia Antipolis Cedex (France)

Unité de recherche INRIA Futurs : Parc Club Orsay Université - ZAC des Vignes
4, rue Jacques Monod - 91893 ORSAY Cedex (France)
Unité de recherche INRIA Lorraine : LORIA, Technopôle de Nancy-Brabois - Campus scientifique
615, rue du Jardin Botanique - BP 101 - 54602 Villers-lès-Nancy Cedex (France)
Unité de recherche INRIA Rennes : IRISA, Campus universitaire de Beaulieu - 35042 Rennes Cedex (France)
Unité de recherche INRIA Rhône-Alpes : 655, avenue de l'Europe - 38334 Montbonnot Saint-Ismier (France)
Unité de recherche INRIA Rocquencourt : Domaine de Voluceau - Rocquencourt - BP 105 - 78153 Le Chesnay Cedex (France)

Éditeur
INRIA - Domaine de Voluceau - Rocquencourt, BP 105 - 78153 Le Chesnay Cedex (France)
http://www.inria.fr
ISSN 0249-6399